Atmospheric Environment 101 (2015) 303–311

Contents lists available at ScienceDirect

Atmospheric Environment

journal homepage: www.elsevier.com/locate/atmosenv

High resolution inventory of GHG emissions of the road transport sector in Argentina

Salvador Enrique Puliafito [a, b, *], David Allende [a], Sebastián Pinto [b], Paula Castesana [b]

[a] Facultad Regional Mendoza, Universidad Tecnológica Nacional/CONICET, Rodriguez 273, 5500 Mendoza, Argentina
[b] Facultad Regional Buenos Aires, Universidad Tecnológica Nacional, Medrano 951, 1179 Buenos Aires, Argentina

HIGHLIGHTS

- A high resolution inventory of road transport emission is presented.
- A better spatial distribution of urban areas is obtained using DMSP-OLS satellite.
- Fuel consumption at district level is spatially reassigned to street segment.
- The proposed GHG emission inventory is compared to international databases.
- The information is organized under GIS environment for air quality models.

ARTICLE INFO

Article history:
Received 14 July 2014
Received in revised form
17 November 2014
Accepted 19 November 2014
Available online 20 November 2014

Keywords:
High resolution emissions inventory
Road transport sector
Geographic information system
Spatial distribution
Vehicle-Kilometer transported
Argentina

ABSTRACT

Air quality models require the use of extensive background information, such as land use and topography maps, meteorological data and emission inventories of pollutant sources. This challenge increases when considering the vehicular sources. The available international databases have uneven resolution for all countries including some areas with low spatial resolution associated with large districts (several hundred km). A simple procedure is proposed in order to develop an inventory of emissions with high resolution (9 km) for the transport sector based on a geographic information system using readily available information applied to Argentina. The basic variable used is the vehicle activity (vehicle – km transported) estimated from fuel consumption and fuel efficiency. This information is distributed to a spatial grid according to a road hierarchy and segment length assigned to each street within the cell. Information on fuel is obtained from district consumption, but weighted using the DMSP-OLS satellite "Earth at night" image. The uncertainty of vehicle estimation and emission calculations was tested using sensitivity Montecarlo analysis. The resulting inventory is calibrated using annual average daily traffic counts in around 850 measuring points all over the country leading to an uncertainty of 20%. Uncertainties in the emissions calculation at pixel level can be estimated to be less than 12%. Comparison with international databases showed a better spatial distribution of greenhouse gases (GHG) emissions in the transport sector, but similar total national values.

1. Introduction

Regional Air Quality Models (RAQM) are mathematical tools used to simulate the physical and chemical processes involving dispersion and reaction of pollutants in the atmosphere which require the preparation of a detailed emissions inventory. Some of the mostly used numerical meteorological and air quality models are WRF/Chem (Grell et al., 2005); CMAQ (Binkowski and Roselle, 2003); CALPUFF (Scire et al., 2000) and AERMOD (Cimorelli et al., 2003).

Input emission inventories necessary for RAQM are usually organized in a chessboard grid associated to a Geographic Information System (GIS). Point sources are associated with large industrial and power generation sources, which are well known data (i.e., emission rate, stack height, exhaust temperature). Area sources are generally associated with specific groups of small residential or diffuse emissions (i.e., material piles, soil erosion, and biogenic

* Corresponding author. Facultad Regional Mendoza, Universidad Tecnológica Nacional/CONICET, Rodriguez 273, 5500 Mendoza, Mendoza, Argentina.
E-mail address: epuliafito@frm.utn.edu.ar (S.E. Puliafito).

http://dx.doi.org/10.1016/j.atmosenv.2014.11.040
1352-2310/

sources among others). Line sources are typically associated (though not exclusively) to vehicular and mobile sources. However, estimating emissions from mobile sources is complex because vehicular traffic composition is inherently random, both temporally and spatially, so mobile sources association with air quality models is a difficult task.

Many scholars have addressed the estimation of emissions from the road transport sector. For example Uherek et al. (2010) reviews the causes and the impacts on air quality and climate generated by road transport, including the mobility problem, emission factors and models currently in use, citing several relevant articles. Several road transportation inventories were prepared in order to estimate national greenhouse gases emissions and to estimate the reduction potential of this sector, mostly compiled by the IPCC (2007).

There are several ways to organize an inventory of emissions based on fuel consumption (i.e. Singer and Harley, 1996; Yan and Crookes, 2009; Hao et al., 2011; among others). Rentziou et al. (2012) and Bastani et al. (2012) present a comprehensive literature review for vehicular activity and fuel consumption models and study the main variables affecting the amount of kilometers driven annually and discuss the uncertainties associated with estimates of transport greenhouse gases (GHG) emissions.

The use of GIS in air quality models can be seen in the initial methodological work of Bruckman (1992), Souleyrette et al. (1992), Bachman (2000) and other works applied to cities and regions: Gualtieri and Tartaglia (1998): Florence, Italy; Borrego et al. (2000, 2003): Lisbon, Portugal, Lin and Lin (2002): Taichung, Taiwan; Puliafito et al. (2003), Mendoza, Argentina; Elbir et al. (2010): Istanbul, Turkey; Puliafito et al. (2011): Bahia Blanca and Buenos Aires, Argentina; Guttikunda and Calori (2013): Delhi, India.

Top-down approaches are used for the estimation of national vehicular emissions inventories (Eggleston et al., 1991). Vehicle activity and emission are estimated using national aggregate data such as the population density, average number of trips and average driving distances, vehicle fleet composition and fuel efficiency. Emission factors are calculated by means of operational models such as COPERT (Ntziachristos and Samaras, 2000); SMOKE (Coats, 1995; Wang et al., 2011); MOBILE6 (MOBILE6, 2001; Zhang and Batterman, 2010); IVE (Davis et al., 2005). D'Angiola et al. (2010), show an example of the application of IVE model for several South American megacities.

In recent years many international air pollutant emissions inventories have been available in various scales. Baldasano et al. (2008) present an emission inventory for Spain and Europe (HERMES) in very high spatial (1 km) and temporal (1 h) resolution used for air quality forecast. Ferreira et al. (2013) present a comparison of several databases on European territory: EMEP (European Monitoring and Evaluation Programme) (EMEP, 2010) and one developed by TNO (Netherlands Organization for Applied Scientific Research) (Denier van der Gon et al., 2010). Ferreira et al. (2013) show that regarding emissions from road transport sector (code SNAP07) there exist major differences especially due to unequal spatial disaggregation and databases used by EMEP and TNO. Macknick (2011) shows that even databases prepared by international organizations such as BP (2010), UN (2010) and IEA (2010) may have up to 9% of discrepancies in primary energy consumption and up to 2.7% in CO_2 emissions from this consumption, due to the methodology and the way national data are reported. TNO developed the EDGAR database (Emissions Database for Global Atmospheric Research) (EDGAR, 2011). EDGAR latest version v4.2, provides global annual emissions data for all air pollutants and GHG disaggregated by countries with a grid resolution of 0.1°. The estimation of these emissions is subject to uncertainties in the activity data from national statistics, adjustments for incomplete time series and the use of general emission factors. Furthermore, if the available geographic data have very coarse resolutions (large districts) the expected global map is of low reliability. Hence, when applying these international databases to RAQM (i.e., ranging from hundreds to thousands of kilometers), the available international databases either do not have always appropriate resolution or are not sufficiently updated. Moreover, not all countries have the same level of disaggregation of information both in quantity, quality or spatial resolution that allows assembling a consistent regional inventory model.

Therefore the purpose of this article is to show a practical top-down methodological approach applied to the development of a geographically distributed high resolution emissions regional inventory of road transportation for Argentina; to improve the existing emissions inventory applicable to a RAQM. While this study was developed for Argentina, its methodological description is transferable to any region or country, using only basic and accessible information for many other countries.

2. Material and methods

2.1. Brief description of the study area

Argentina is located in the southern part of South America. It has 40 million inhabitants and covers an approximate area of 2,800,000 km^2 of continental and insular territory. In 2012 the gross domestic product (GDP) was 470 million USD (at current prices) with an annual GDP/capita of 11,500 USD. The country is divided into 23 provinces and an autonomous city. The provinces are in turn organized into municipalities totaling 537 districts. Of the latter, 48% have less than 25,000 inhabitants representing 7% of the total population; 37% have between 25,000 and 150,000 inhabitants (29% total population), and the remaining 15% have 150,000 representing 64% of the total population (Table 1). The vehicle fleet reaches 11.5 million units in 2012, with an annual fuel consumption of 8.8 million m^3 of diesel oil, 6.5 million m^3 of gasoline and 2000 million m^3 of compressed natural gas (CNG) (Supl. inform. Table A.1 and A.2). The road network reaches approximately 500,000 km, of which 38,000 km are highways (90% paved), 200,000 km are primary and trunk roads (20% paved) and 270,000 km are secondary and tertiary roads mostly unpaved. Table A.3 (supl. inform.) show the references for the databases used in this text (INDEC, ADEFA, DNVA, SENA, STNA, IGNA, OpenStreet Map, among others). According to the GHG national inventories presented by Argentina to the IPCC (Argentina, 2007) from a

Table 1
Fuel consumption by district size in the year 2012.

Population range	Total thousand inhab.	Diesel oil thousand m^3	Gasoline thousand m^3	NCG thousand m^3
Pop. < 25,000	2,850	892	487	48,108
25,000 < pop. < 150,000	11,538	3,843	1,993	487,719
Pop. > 150,000	25,729	4,457	4,369	1,619,202
Total	40,117	9,192	6,849	2,155,029
Population range	**Proportion**	**%**	**%**	**%**
Pop. < 25,000	7%	10%	7%	2%
25,000 < pop. < 150,000	29%	42%	29%	23%
Pop. > 150,000	64%	48%	64%	75%
Total	100%	100%	100%	100%
Population range	**Consumption**	**l/Inhab.**	**l/Inhab.**	**m^3/Inhab.**
Pop. < 25,000		313.0	170.9	16,880
25,000 < pop. < 150,000		333.1	172.7	42,271
Pop. > 150,000		173.2	169.8	62,933
Total		229.1	170.7	53,719

sectorial point of view, annual CO_2 eq. emissions (for year 2000) correspond: 132 Tg to energy, 125 Tg to agriculture, 11 Tg to industry, 14 Tg to waste, while land use changes and forestry captures 43 Tg, adding 239 Tg. Transport sector emits 43 Tg contributing to 32% of the energy uses and 18% of total emissions.

2.2. Basic data structure

The inventory was prepared using a geographical information system (GIS). Databases were organized with the following primary information (Fig. 1): a) Maps of urban localities, fuel sales at urban locations and Annual Mean Daily Traffic (AMDT) at control points in trunk roads. b) Map of Argentina by district with information on population density; c) Streets and roads maps: main city access, trunk routes, national highways, provincial roads, primary and secondary streets. d) Satellite image DMSP-OLS "*Earth at night*" (EAN) with three bands intensities: Red, Green and Blue (R, G, and B) (NOAA-NGDC, 2010).

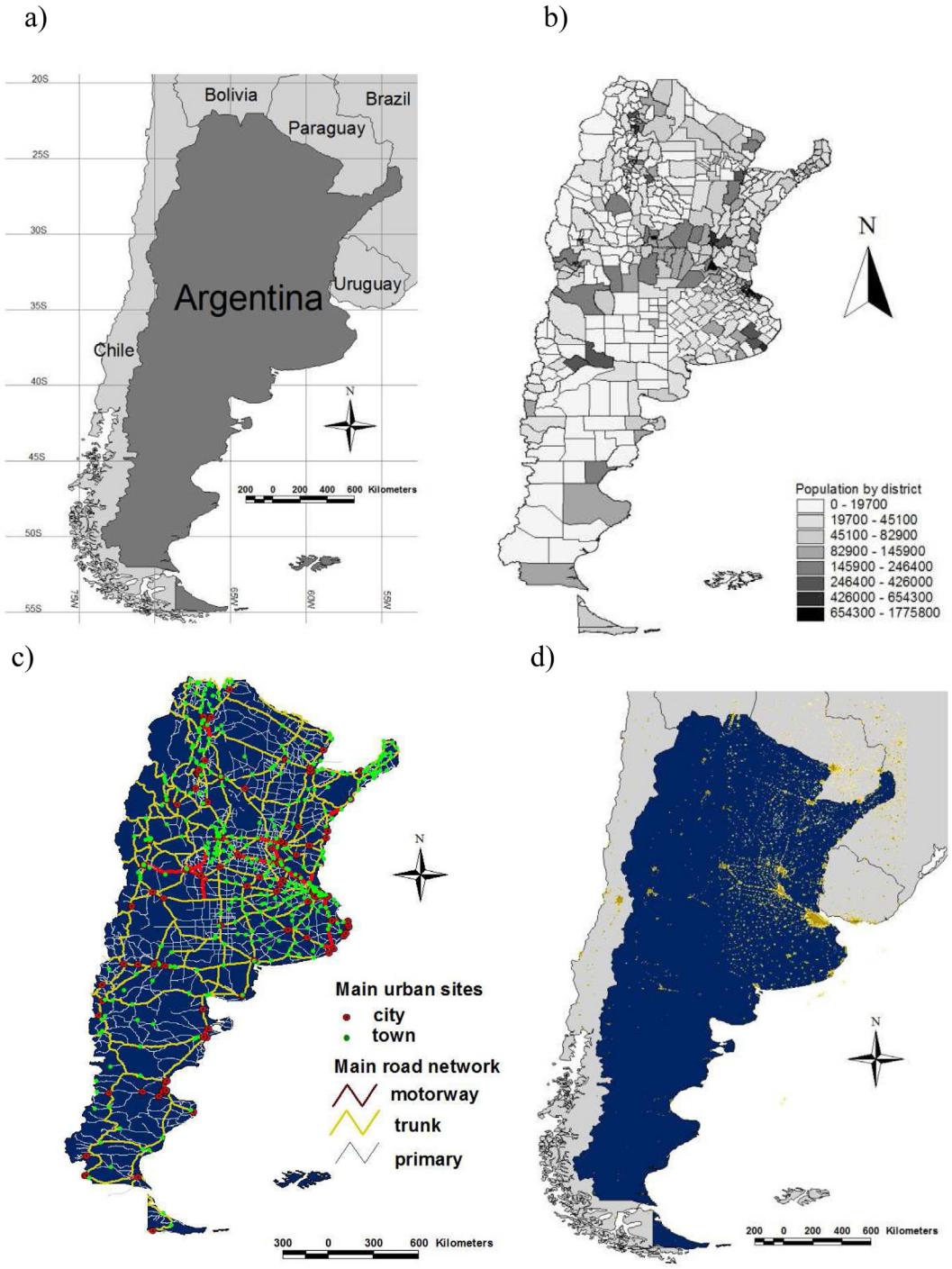

Fig. 1. Initial geographically referenced information using different types of representation in GIS shape format: a) Map of continental Argentina in South America; b) Argentine population by districts (Polygon shape); c) Location of Cities and Towns (point shape); and main access routes (line shape); d) Night lights ("Earth at night").

2.3. Data processing

2.3.1. Grid resolution

Forecasting and managing urban air quality, especially determining the impact of near-source impacts of line sources cannot be properly resolved with large grids (>15 km). But a higher resolution does not necessarily imply improvements in the prediction skills (Mass et al., 2002). There are several studies that investigate the differences in the model predictions as the model resolution is increased showing that depending on the type of pollutant, a 36 or a 12 km grid spacing predict concentrations with roughly the same error, although there are improvements with the use of higher resolutions ($\approx$4 km) (Ching et al., 2006; Fountoukis et al., 2013).

From a methodological point of view, the highest spatial resolution, for the here proposed emission inventory is 1 km, since this is the resolution of the EAN image. However we would choose this very high resolution (1 km) for air quality assessment at an urban scale of typically of 100–500 km, where it could be possible to calibrate vehicular fluxes and use fuel sales at a finer grid resolution (i.e., 3 km or 1 km). Nevertheless for an extended area such as Argentina a resolution of 9 km already produces a relative high resolution inventory; on the other hand when using WRF/Chem for Argentina regional calculations we use three steps downscaling typically of 27–9–3 km. Therefore for the present study we chose a rectangular grid covering Argentina (1700 km E–W direction and 3800 km N–S direction), with cells of 9 × 9 km resolution as the basic structure for information storage (Fig. 2a).

2.3.2. Distribution of population by cell

The best publicly available population density and other demographic variables are included at district level, which normally are larger than the size of the grid cell. Although there is a map of urban locations represented as a point; however, it does not include urban boundaries. Urban boundaries could be defined by street segments density but they are not equally present for the entire Argentine national map. Therefore urban centers as major emitters were associated to the red band from EAN. Doll et al. (2006), Levin and Duke (2012) justify the use of these images to determine socio-demographic variables. The satellite image EAN (Fig. 1d) was converted to a polygon shape and then intersected with the base grid. Likewise population data (Fig. 1b) was intersected with the base grid incorporating the available population and socio-economic data for each district. District m population is distributed according to the intensity of the red band $B_R(x, y, m)$, included in the base grid.

$$Pob_{GRID}(x,y) = Pob_{DT}(m) \times \frac{B_R(x,y,m)}{\sum_{x,y} B_{R(x,y,m)}} \quad (1)$$

where $Pob_{GRID}(x, y)$ (Fig. 2b) is the population assigned to the cell at coordinates (x, y) and $Pob_{DT}(m)$ is the population of each district m (Fig. 1b). B_R varies from 0 for open areas (no lights) to a maximum of 0.8 at urban centers. Green band was not used since it is mostly associated to streets and highway illumination defining a contour larger than the urban boundaries as seen from visible satellite images as Google-Earth or Landsat. On the other hand, B_R defined the city boundaries better. Blue band represents open areas (mountain, sea or rural sites).

2.3.3. Consumption per cell

The basic information on fuel sales ($Fuel_{DT}$) (Supl. inform. Table A.1) is obtained at the district level (m). Similarly to the distribution of the population at the grid level fuel consumption ($Fuel_{GRID}$) is estimated as:

$$Fuel_{GRID}(x,y,i) = Fuel_{DT}(m,i) \times \frac{B_R(x,y,m)}{\sum_{x,y} B_{R(x,y,m)}} \quad (2)$$

where subscript i indicates the type of fuel (gasoline, diesel or CNG). Table 1 shows fuel consumption compared to district population size. It is observed that the consumption of gasoline and CNG is almost proportional to the district population, its per capita consumption varies only slightly with respect of district size; however it is not true for diesel oil since it involves freight transport. Per

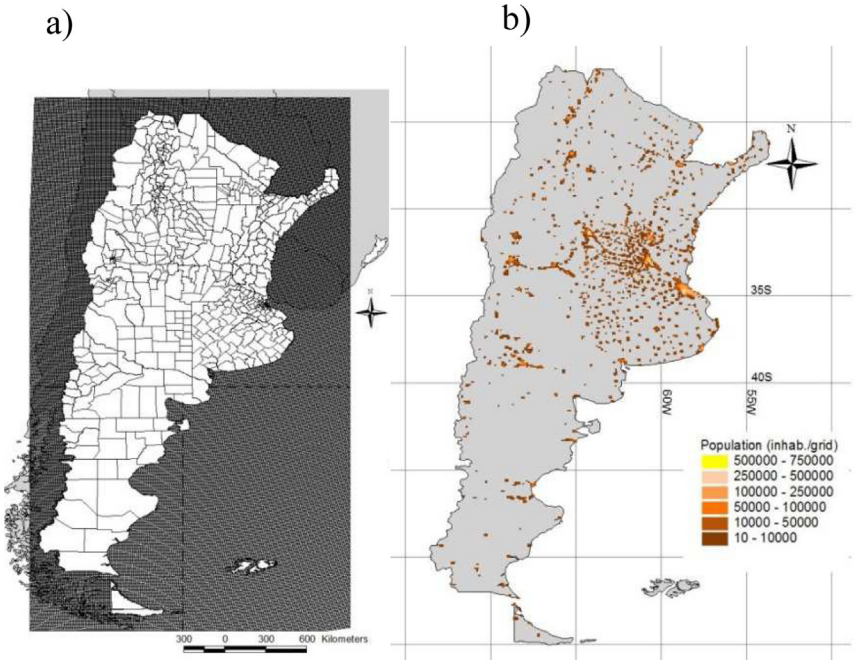

Fig. 2. a) 9 km resolution grid shape over the Argentine territory; b) Population at grid level $Pob_{GRID}(x,y)$.

capita consumption of CNG is higher in more populous urban districts, due to the higher presence of gas stations.

2.3.4. Redistribution of consumption per cell

It is assumed that not all fuel sold or assigned to the cell ($Fuel_{GRID}$) is completely consumed in the same cell, but as vehicles move, they partially consume their fuel from neighboring cells. Vehicle traffic rate is proportional to the population density of each urban center. Therefore $Fuel_{GRID}$ consumption per cell is distributed through a point spread function (i.e., Mertens and Replogle, 1977), which is the convolution of $Fuel_{GRID}$ with a bi-Gaussian filter function $bg(x,y)$. In this case a filter function of 15 × 15 cells was used with a deviation d (variable for each fuel type) and maximum values in x_m and y_m:

$$bg(x,y) = \exp\left[-\left(\frac{x-x_m}{d}\right)^2\right] \times \exp\left[-\left(\frac{y-y_m}{d}\right)^2\right] \quad (3)$$

where $bg(x_m, y_m) = 1$.

$$Fuel_{CONV}(x,y,i) = \frac{1}{\sum_{u,v} bg(u,v)} \iint_{u=u_0,v=v_f}^{u=u_f,v=v_f} [Fuel_{GRID}(u,v,i) \times bg(x-u, y-v)]\,du\,dv \quad (4)$$

$Fuel_{CONV}$ is the proportion of the fuel consumed (or distributed) in each cell of coordinates (x,y); $u_{f,0} = x \pm x_m/2$; $v_{f,0} = y \pm y_m/2$. This step is necessary, otherwise rural routes or cells would appear with no consumption or an underestimated consumption, while urban cells would appear with an overestimated consumption. The width of the filter function can be set for each fuel type $d(i)$. Freight transport using diesel oil had a wider distribution. This value is calibrated with the daily flow rate as explained below.

2.3.5. Total domestic activity

In order to calibrate the model with data from road AMDT, it is necessary to estimate VKT (vehicle km transported) activity by fuel type. This is calculated through fuel sold by jurisdiction and estimating average fuel efficiency γ, i.e., traveled km/liters per vehicle and fuel type i (ADEFA, Yearbook 2012) (Table 2):

$$VKT_{DT}(m,i) = Fuel_{DT}(m,i) \times \gamma(i) \quad (5)$$

2.3.6. Activity at cell and segment level

Similarly we can determine the activity of each cell VKT_{GRID} from the fuel assigned to each cell $Fuel_{CONV}$ using Eq. (5).

$$VKT_{GRID}(x,y,i) = Fuel_{CONV}(x,y,i) \times \gamma(i) \quad (6)$$

Table 2
Average annual national activity in the year 2012.

Variable/fuel	Units	Gasoline	Diesel oil	NCG	Total
Registered number of vehicles	Thousands	5237	4444	1796	1477
Percentage of vehicles	%	46	39	16	100
Fuel consumption	Thousand m^3	6,849	9,193	2,155*	
Fuel efficiency	km/l	11	9	14**	
Annual VKT	Millions veh.-km	75,340	82,734	30,170	188,245
Percentage of VKT	%	42	39	19	100
Daily traveled distance per vehicle	km	39	51	46	

Ref.: VKT: Vehicle-km traveled, NCG: Natural Compressed Gas. (*) NCG consumption in millions m^3; (**) NCG efficiency in km/Thousand m^3.

However since the actual consumption is done on the routes it is necessary to transfer the information from the grid to the segment level by intersecting the line shape with the grid shapes.

The activity in each segment is $VKT_{SEGM}(s,i) = VEH_{SEGM}(s,i) \times L(s)$; being VEH_{SEGM} the vehicles using fuel i at the segment s, and being L the length of that segment. Streets segments were classified into main access, trunk routes, primary routes, secondary and tertiary roads. One cell has a single activity value VKT_{GRID}, but in each cell coexists s segments of different lengths and hierarchies. Note that $VKT_{GRID}(x,y,i) = \sum_s VKT_{SEGM}(s,i)$ is the activities summation of all segments s. However, usually, there is no information on the average daily vehicles for each segment; therefore this information must be estimated from the consumption of the cell and the hierarchy of the routes. Thus the segment hierarchy is used as a proxy for segment vehicles flux:

$$VKT_{GRID} = \sum_S VEH_{REF} \times J(s) \times L(s); \quad (7)$$

and

$$VEH_{REF} = VKT_{GRID} \Big/ \sum_S \times J(s) \times L(s) \quad (8)$$

which means for example that the amount of vehicles in a given segment is $J(s)$ times the reference number of vehicle VEH_{REF}. Coefficient $J(s)$ takes into account traffic flow and use of the road, and can be estimated using measuring flow points AMDT. Table 3 shows the average AMDT for different roads classes in Argentine roads. Assuming a VEH_{REF} = 120,000, then main access and motorways close to urban centres are considered with hierarchy #1 and it is given a coefficient or ratio $J(1) = 1$ (ratio = Assumed/VEH_{REF}). Motorways are represented with 2 segments in the GIS map, so each segment receives an equal assignment of daily traffic. National roads connecting big urban centres (>150,000 inhab.) are given the hierarchy #2 and $J(2) = 0.25$; primary roads connecting medium size urban centres (>25,000 inhab. and <150,000 inhab.), are given the hierarchy #3 and $J(3) = 0.075$. Roads connecting small urban centres (<25,000 inhab.) in the rural area are considered with hierarchy #4, $J(4) = 0.033$. Secondary and tertiary streets area rural roads with very low traffic flow are given hierarchies 5 and 6 respectively. Note that the hierarchy also determines the speed and average fuel consumption for each category of vehicle. Speed of traffic flow and vehicle type are both measured in around 30% of the AMDT control points across the country, but it is not available for motorways. Table A.4 (Supl. inform.) shows average speed and vehicle proportions at rural roads measured at selected AMDT control points. COPERT model assigns for light vehicles class: 25–45 km/h for urban roads; 50–80 km/h rural roads and 85–115 km/h for highways. In comparison rural argentine roads

Table 3
Average AMDT according to segment hierarchy.

Hierarchy and road class	Number of points	AMDT			Ratio
		Average	Std. dev.	Assumed	
1 Motorways	55	112,890	55%	120,000(*)	1.000
2 National trunk roads	229	29,961	38%	30,000	0.250
3 Primary roads	243	9,763	24%	9,000	0.075
4 Provincial roads	570	3,838	32%	4,000	0.033
5 Secondary streets	336	1,281	32%	1,000	0.008
6 Tertiary streets	115	243	56%	250	0.002

AMDT: Annual mean daily traffic; (*)VEH_{REF} = 120,000; ratio = Assumed/VEH_{REF}.

presents an average of 96 km/h for light vehicles and 76 km/h for heavy vehicles. Urban average speed reaches 39 km/h considering a time share of 20% in urban highways, 20% in main roads, 30% in residential streets and 30% in downtown main streets (Puliafito et al., 2010).

The activity of the segment is proportional to VKT_{GRID} and weighted by the average of the product of the road hierarchy $J(s)$ and the length of $L(s)$ at segment s for each grid.

$$VKT_{SEGM}(s,i) = VKT_{GRID}(x,y,i) \times J(s) \times L(s) \Big/ \left[\sum_{S} \times J(s) \times L(s)\right] \quad (9)$$

Once VKT_{SEGM} is calculated, the daily average vehicles VEH_{SEGM} is determined in each segment dividing VKT_{SEGM} by the segment length $L(s)$. This value allows us to compare the results with existing AMDT values. The width d of the bigaussian function in Eq. (3) can be calculated by iterating Eqs. (3), (4), (6) and (7). Since emissions depend on the vehicle fuel and type, an adequate distribution of vehicle is required. Being $Sh(i,z)$ the distribution of vehicle by type z and fuel i (Table 4), then vehicle at street levels are distributed as:

$$V_{SEGM}(s,i,z) = VEH_{SEGM}(s,i)*Sh(i,z) \quad (10)$$

Nationwide fuel use is 45% gasoline, 15% CNG and 35% Diesel-Oil (ADEFA, Yearbook 2012).

2.3.7. Emissions by jurisdiction cell and segment

The above process allows us to calculate vehicular emissions at cell, segments or district level. The emissions E_{DT} for pollutant k, was calculated for a given fuel type i at district m (nation, province or district) using an average fuel bulk emission $F_{EF}(k,i)$:

$$E_{DT}(m,k) = \sum_{i}[Fuel_{DT}(m,i) \times F_{EF}(k,i)] \quad (11)$$

Similarly, at grid level:

$$E_{GRID}(x,y,k) = \sum_{i}[Fuel_{GRID}(x,y,i) \times F_{EF}(k,i)] \quad (12)$$

Using the vehicular activity, the emissions are calculated using an activity emission factor

$$E_{DT}(m,k) = \sum_{i}[VKT_{DT}(m,i) \times A_{EF}(i,z,k)] \quad (13)$$

$$E_{GRID}(m,k) = \sum_{i}[VKT_{GRID}(m,i) \times A_{EF}(i,z,k)] \quad (14)$$

Activity emission factors are specific for vehicle type and fuel. For small scales or short termed inventories it is possible to include an hourly variation coefficient that considers time dependence (Baldasano et al., 2008).

At segment level emissions are calculated as follows:

$$E_{SEGM}(s,k) = \sum_{j,i,z}[VKT_{SEGM}(s,i,z) \times A_{EF}(i,z,k)] = \sum_{j,i,z}[V_{SEGM}(s,i,z) \times L(s) \times A_{EF}(i,z,k)] \quad (15)$$

Each segment has the identification of the cell to which it belongs; therefore emissions per segment can be reassigned to the grid. Therefore the cell emission is the sum of emissions from all segments s:

$$E_{GRID}(k,x,y) = \sum_{s} E_{SEGM}(s,k) \quad (16)$$

Finally the total (national) emissions by pollutant may be aggregated by districts, segments or cells:

$$E(k) = \sum_{x}\sum_{y} E_{GRID}(k,x,y) \quad (17)$$

while emissions from Eq (11) are calculated based on fuel sales in the cell, Eq. (15) is carried out based on vehicle type discrimination at the segment level in each cell. This calculation is usually performed in bottom-up models based on vehicle counts in the streets (as in the HERMES model, Baldasano et al., 2008). In Eq. (12) we could have used $Fuel_{CONV}$, however this distribution is used to assign vehicular traffic on the segments, since there may be cells with positive values of $Fuel_{CONV}$, due to dispersal effect of the convolution, with no route segments associated to that cell. This is particularly true in large rural areas of central and southern Argentina.

3. Results

Fig. 3a) shows the distribution of fuel $Fuel_{CONV}$ calculated with Eq. (4). From this figure vehicular activities are allocated at grid and segment level (seen as a GIS layer). Fig. 3b) shows a detail of central Argentina for the assigned vehicles per segment according to type and hierarchical routes. Thicknesses and colors indicate greater or lesser amount of traffic. Table 4 resumes the distribution of transport emissions according to the hierarchy of the route. It is noted that 46% of all emissions are developed on motorways and trunk routes, and 30% are developed in urban areas. Emissions of pollutants emitted by combustion such as CO, CH_4 and NOx (among others) can be estimated using the appropriate emission factor $F_{FE}(k, i)$ according to Eq. (12).

3.1. Calibration and sensitivity calculations

By spreading the fuel consumption (Eq. (4)) some values may be distributed to neighbor countries or over the ocean. The missing fuel values were less than 3% depending on the width of the spread function. Although, the first case could be considered as transboundary traffic, we compensated the missing values by adjusting the total national emissions in Eq (14) to be equal to Eq (13).

Also the convolution function may assign fuel consumption to cells with no street segments; therefore after computing vehicles in each segment, we force Eq (16) to be equal to Eq. (13), by increasing a fixed proportion the amount of vehicles in each segment. In this way only cells with street segments have traffic emissions. The differences before compensating were less than 12%.

We checked the vehicle assignments in each segment using 848 AMDT measuring points all over the country for different road

Table 4
CO_2 emissions according to road hierarchy (Gg/year) in the year 2012.

Hierarchy/Fuel	# Seg.	Length	NCG	G	DO	Total	Urban	Rural
Motorways	7,538	7,922	1,552	3,233	5,463	10,271	20%	3%
Trunk roads	12,514	38,317	1,026	3,072	5,755	9,854	10%	13%
Primary roads	25,800	78,011	1,530	4,412	8,217	14,167	13%	19%
Secondary roads	29,617	39,077	1,050	2,958	5,227	9,247	11%	10%
Others	2,933	5,275	42.1	128.3	243.2	413.6	0%	1%
Total	78,402	168,602	5,202	13,805	24,907	43,954	54%	46%

Ref.: NCG: Compressed Natural Gas; G: Gasoline; DO: Diesel-Oil; # Seg.: Number of segments; Length: Total segment length (km).

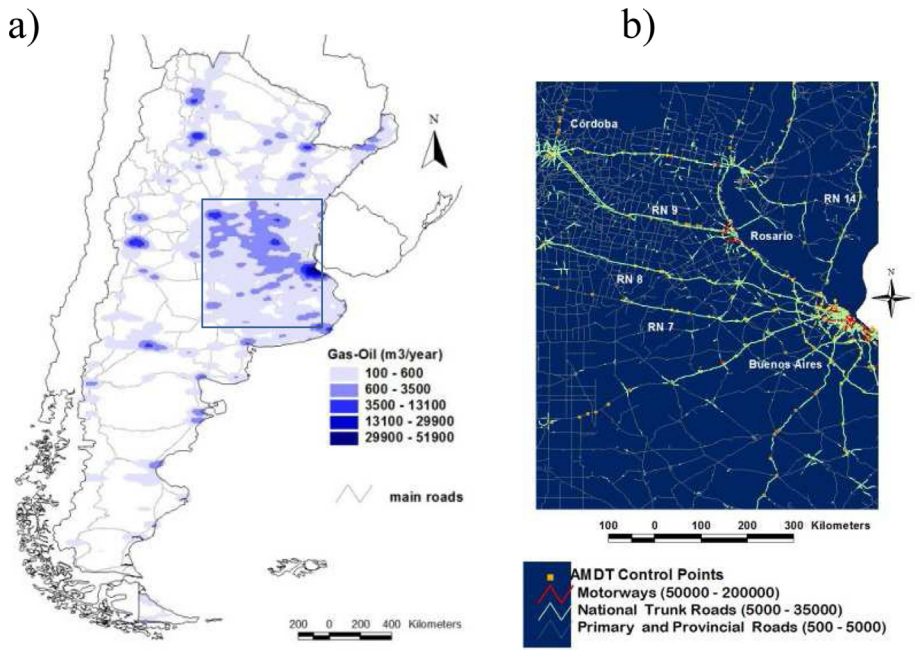

Fig. 3. a) Diesel-oil consumption (m^3/year) distribution according to $Fuel_{CONV}$; b) Detail of the Buenos Aires – Rosario-Córdoba area with roads hierarchy (RN: National Roads), AMDT control points and traffic flow range of VEH_{SEGM}.

hierarchies (Fig. 3b). To test the sensitivity of calculations we performed a Montecarlo analysis by assuming uncertainties of the following coefficients: a) ±60% the width of the filter function *d* (Eq. (3)); b) ± 30% fuel efficiency γ (Eq (5)) and c) ±50% hierarchy weights *J*. In each run the coefficients were selected using a uniform random function. The average of more than 100 tries showed an uncertainty in vehicle assignment of 22% with a correlation factor of 0.95 (Fig. 4a). Fig. 4b depicts the frequency distributions for both calculated and measured traffic flows, showing that AMDT values are mainly distributed below 15,000 veh./day corresponding to rural areas, while higher values are present in highways segments close to urban areas.

Fig. 5 show the effect of changing the spread coefficient *d* on the estimation of daily vehicle flow on National Route RN9, compared to its AMDT values. The slope of the function is used to find the proper value for coefficient *d*.

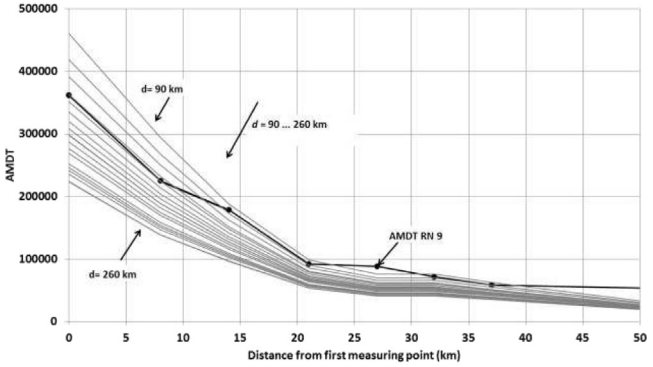

Fig. 5. AMDT values (black line) and estimated values (gray lines) for National Road RN 9 for different values (90–260 km, step: 9 km) of the spread coefficient *d* in Eq (3).

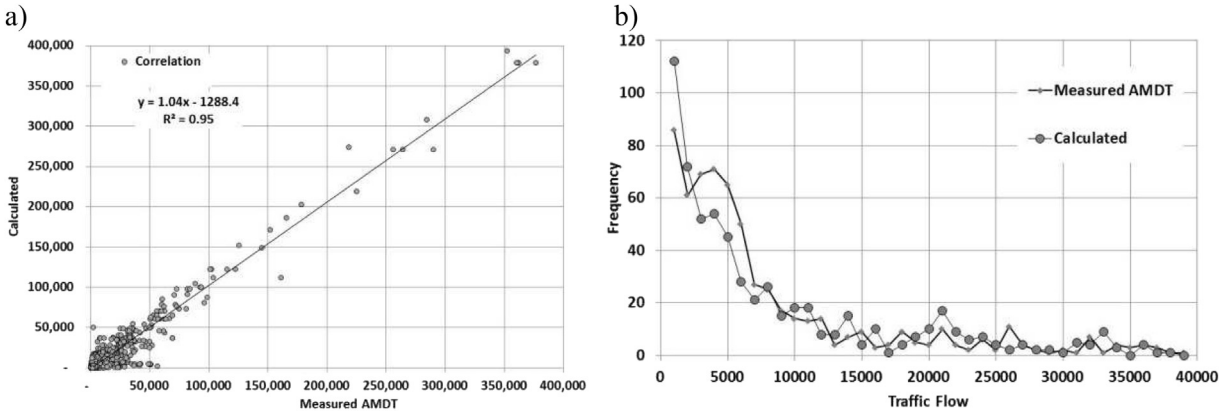

Fig. 4. a) Correlation of calculated vs. measured traffic flows at 848 segments; b) frequency distribution of measured and calculated AMDT flow.

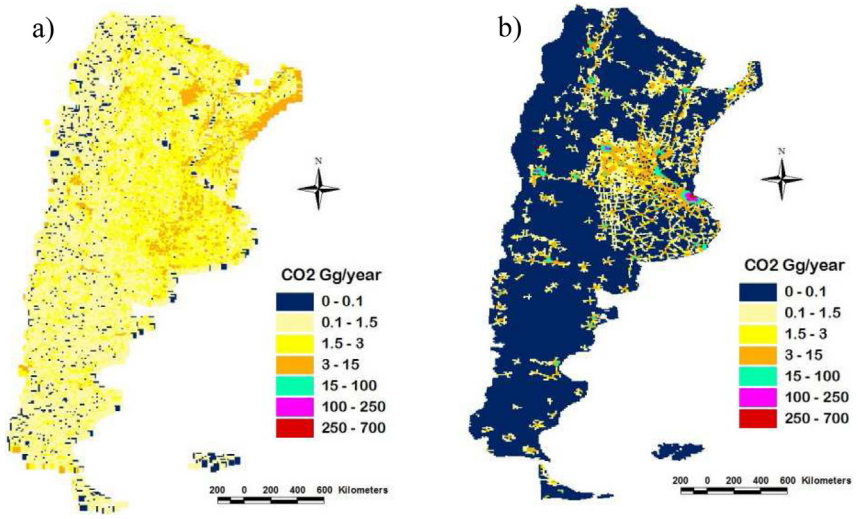

Fig. 6. Annual CO_2 emission map at the grid layer for road transport sector; a) EDGAR SNAP07; b) present work.

4. Discussion and conclusions

The air quality models require the use of extensive background information, such as land use/land cover maps, topography, meteorological data and emission inventories. In regional models, preparation of such databases is a real challenge due to the involved scales (hundreds to thousands of km) and also due to the scarcity of available organized data. International emission databases not always have the same resolution for all nations since they are built from national available statistics. In many cases they may even have very low spatial resolution associated to data from large districts (hundreds of km). Fig. 6a shows the EDGAR (SNAP07) inventory from the road transport sector for Argentina. If compared with Fig. 6b (this study) it can be seen that the spatial distribution is not similar although total emissions calculated by EDGAR for Argentina (36,800 Gg in the year 2010) vary only by 15% according to this study (43,950 Gg in the year 2012). The difference is that EDGAR distribution has 99% of the cells below 5 Gg/year and 1% of the cells range between 5 and 15 Gg/year, and only 16% of the cells are below 0.5 Gg/year (Fig. A.1 supl. inform.). The spatial distribution of CO_2 emission in EDGAR map could be associated to the use of large districts population density. In our study, 88% pixels are under 5 Gg/year, 8% range between 5 and 15 Gg/year and few cells (3%) range between 15 and 700 Gg/year. This remaining 3% of higher values (>15 Gg/year) correspond to the emissions (of CO_2) in big urban centers. On the other hand, for the lowest values in our study, 50% of the cells, corresponding mostly to rural areas, are below 1 Gg/year. While EDGAR distribution is more uniform throughout the country, the CO_2 emissions in this study are mostly concentrated around urban centers. To estimate traffic flow EDGAR uses a proxy under the concept of segment length $\times$ population, varying linearly between a minimum value for rural areas and a maximum value for urban areas (Janssens-Maenhout et al., 2012), assuming that vehicular flux density increases as it approaches urban centers.

For the purposes of the methodology proposed in this article, the basic variable is the vehicular activity vehicle-kilometers transported (VKT), estimated from fuel consumption per grid and fuel efficiency. This information is then distributed according to a road hierarchy and the length of the street segment. The basic fuel consumption is obtained at the district level, but it is weighted by the red band of DMSP-OLS satellite image "Earth at night". In order to distribute this consumption in rural areas, fuel consumption is spread with a bigaussian function, which implicitly considers that traffic flows are stronger near the urban areas and lower as they move away from them. The uncertainty of vehicle estimation using 848 measuring daily traffic fluxes is less than 25%. Uncertainties in the emissions calculation at pixel level can be estimated to be less than 12%.

Finally it should be noted that although the basic grid is of 9 $\times$ 9 km, since the vehicular flux is distributed at the segment level, it is possible to generate maps of higher spatial resolution, especially for its use in air quality for local or regional scale. From a methodological point of view the lower limit for the spatial resolution is 1 km, since this is the resolution of the DMSP-OLS satellite "Earth at night" image, but this will depend on the availability of basic information at finer grid resolution. In fact, for Argentina we would choose this resolution (1 km) for a smaller area, for example at the urban regional scale of 100–200 km, where it could be possible to calibrate vehicular fluxes and fuel sales at a finer grid resolution (i.e., 3 km or 1 km). In subsequent studies finer resolution inventories will be prepared including other sources of emissions, which will be included in this Atlas of Argentina.

Acknowledgments

The authors would like to thank Universidad Tecnológica Nacional (UTN) (National Technological University) and Consejo Nacional de Investigaciones Científicas y Técnicas (CONICET) (National Council for Scientific and Technical Investigations) for supporting research activities. This work is granted by UTN IFI Projects PID 1799 and 1487 and CONICET PIP 112 201101 00673.

Appendix A. Supplementary data

Supplementary data related to this article can be found at http://dx.doi.org/10.1016/j.atmosenv.2014.11.040.

References

Argentina, 2007. Second National Report to IPCC. www.ambiente.gov.ar (last accessed 21.10.14.).

Bachman, W., Sarasua, W., Hallmark, S., Guensler, R., 2000. Modeling regional mobile source emissions in a geographic information system framework. Transp. Res. Part C 8, 205–229.

Baldasano, J.M., Güereca, L.P., López, E., Gassó, S., Jimenez-Guerrero, P., 2008. Development of a high-resolution (1 km $\times$ 1 km, 1 h) emission model for Spain: the high-elective resolution modelling emission system (HERMES). Atmos. Environ. 42, 7215–7233.

Bastani, P., Heywood, J., Hope, C., 2012. The effect of uncertainty on US transport-related GHG emissions and fuel consumption out to 2050. Transp. Res. Part A 46, 517–548.
Binkowski, F.S., Roselle, S.J., 2003. Models-3 Community Multiscale Air Quality (CMAQ) model aerosol component 1. Model description. J. Geophys. Res. Atmos. 108 (D6), 4183.
Borrego, C., Tchepel, O., Barros, N., Miranda, A., 2000. Impact of road traffic emissions on air quality of the Lisbon region. Atmos. Environ. 34, 4683–4690.
Borrego, C., Tchepel, O., Costa, A., Amorim, J., Miranda, A., 2003. Emission and dispersion modeling of Lisbon air quality at local scale. Atmos. Environ. 37, 5197–5205.
BP, 2010. British Petroleum Statistical Review of World Energy. BP, London, UK.
Bruckman, L., Dickson, R.J., Wilkonson, J.G., 1992. The use of GIS software in the development of emissions inventories and emissions modeling. In: Proceedings of the Air and Waste Management Association. Pittsburgh, PA.
Ching, J., Herwehe, J., Swall, J., 2006. On joint deterministic grid modeling and sub grid variability conceptual framework for model evaluation. Atmos. Environ. 40, 4935–4945.
Cimorelli, A.J., Venkatram, A., Weil, J.C., Paine, R., Wilson, R., Lee, R., 2003. AERMOD: Description of Model Formulation. Environmental Protection Agency.
Coats, C., 1995. High Performance Algorithms in the Sparse Matrix Operator Kernel Emissions Modeling System. Microelectronics Center of North Carolina, Environmental Systems Divisions.
D'Angiola, A., Dawidowski, L., Gómez, D., Osses, M., 2010. On-road traffic emissions in a megacity. Atmos. Environ. 44, 483–493.
Davis, N., Lents, J., Osses, M., Nikkila, N., Barth, M., 2005. Development and application of an international vehicle emissions model. Transp. Res. Rec. 51–59.
Denier van der Gon, H., Visschedijk, A., Van de Brugh, H., Dröge, R., 2010. A high resolution European emission data base for the year 2005. In: A Contribution to UBA-Projekt: "Strategien zur Verminderung der Feinstaubbelastung" e PAREST: Partikelreduktionsstrategien e Particle Reduction Strategies. TNO report. TNO-034-UT-2010e01895_RPT-ML.
Doll, C., Muller, R., Morley, J., 2006. Mapping regional economic activity from night-time light satellite imagery. Ecol. Econ. 57, 75–92.
EDGAR, 2011. Emissions Database for Global Atmospheric Research. http://edgar.jrc.ec.europa.eu/.
Eggleston, H., Gaudioso, D., Gorissen, N., Joumard, R., Rijkeboer, R.C., Samaras, Z., Zierock, K., 1991. CORINAIR Working Group on Emission Factors for Calculating 1990 Emissions from Road Traffic. In: Methodology and Emission Factors, vol. 1. Commission of the European Communities, DG XI–EEA Task Force, Brussels, Belgium. Contract Number B4–3045 (91) 10PH.
Elbir, T., Mangir, N., Kara, M., Simsir, S., Eren, T., Ozdemir, S., 2010. Development of a GIS-based decision support system for urban air quality management in the city of Istanbul. Atmos. Environ. 44, 441–454.
EMEP, 2010. Emissions Used in EMEP Models. Centre on Emission Inventories and Projections. http://www.ceip.at/emission-data-webdab/emissions-used-inemep-models/.
Ferreira, J., Guevara, M., Baldasano, J., Tchepel, O., Schaap, M., Miranda, A., Borrego, C., 2013. A comparative analysis of two highly spatially resolved European atmospheric emission inventories. Atmos. Environ. 75, 43–57.
Fountoukis, C., Koraj, D., Denier van der Gon, H., Charalampidis, P., Pilinis, C., Pandis, S., 2013. Impact of grid resolution on the predicted fine PM by a regional 3-D chemical transport model. Atmos. Environ. 68, 24–32.
Grell, G.A., Peckham, S.E., Schmitz, R., McKeen, S., Frost, G., Skamarock, W.C., Eder, B., 2005. Fully coupled "online" chemistry within the WRF model. Atmos. Environ. 39, 6957–6975.
Gualtieri, G., Tartaglia, M., 1998. Predicting urban traffic air pollution: a GIS framework. Transp. Res. Part D 3 (5), 329–336.
Guttikunda, S., Calori, G., 2013. A GIS based emissions inventory at 1 km × 1 km spatial resolution for air pollution analysis in Delhi, India. Atmos. Environ. 67, 101–111.
Hao, H., Wang, H., Ouyang, M., 2011. Fuel conservation and GHG (Greenhouse gas) emissions mitigation scenarios for China's passenger vehicle fleet. Energy 36, 6520–6528.
IEA, 2010. International Energy Agency. CO2 Emissions from Fuel Combustion. IEA, Paris, France.
IPCC, 2007. In: Pachauri, R.K., Reisinger, A. (Eds.), Climate Change 2007. Synthesis Report. Contribution of Working Groups I, II and III to the Fourth Assessment Report of the Intergovernmental Panel on Climate Change. IPCC, Geneva, Switzerland.
Janssens-Maenhout, G., Pagliari, V., Guizzardi, D., Muntean, M., 2012. Global Emission Inventories in the Emission Database for Global Atmospheric Research (EDGAR) – Manual (I). Joint Research Centre of the European Commission JRC Technical Reports. http://edgar.jrc.ec.europa.eu/index.php.
Levin, N., Duke, Y., 2012. High spatial resolution night-time light images for demographic and socio-economic studies. Remote Sens. Environ. 119, 1–10.
Lin, M., Lin, C., 2002. The application of GIS to air quality analysis in Taichung City, Taiwan, ROC. Environ. Model. Softw. 17, 11–19.
Macknick, J., 2011. Energy and CO_2 emission data uncertainties. Carbon Manag. 2 (2), 189–205.
Mass, C., Ovens, D., Westrick, K., Colle, B., 2002. Does increasing horizontal resolution produce more skillful forecasts? Bull. Am. Meteorol. Soc. 83, 407–430.
Mertens, L., Replogle, F., 1977. Use of point spread and beam spread functions for analysis of imaging systems in water. J. Opt. Soc. Am. 67 (8), 1105–1117.
MOBILE6, 2001. Fleet Characterization Data for MOBILE6. EPA 420-R-01-047. http://www.epa.gov/oms/models/mobile6/r01047.pdf.
NOAA-NGDC, 2010. Version 4 DMSP-OLS Nighttime Lights Time Series. http://www.ngdc.noaa.gov/dmsp/downloadV4composites.html.
Ntziachristos, L., Samaras, Z., 2000. COPERT III Computer Programme to Calculate Emissions from Road Transport Methodology and Emission Factors. Technical Report No 49. EEA, Copenhagen. Openstreet Map. Free Open Source Maps of the World. http://www.openstreetmap.org.
Puliafito, S.E., Guevara, M., Puliafito, C., 2003. Characterization of urban air quality using GIS as management system. Environ. Pollut. 122, 105–117.
Puliafito, S.E., Gantuz, M., Puliafito, J.L., 2010. Characterizing mobile emissions by on-board measurements. Int. J. Appl. Environ. Sci. 5 (2), 297–316.
Puliafito, S.E., Allende, D., Fernandez, R., Castro, F., Cremades, P., 2011. New approaches for urban and regional air pollution modelling and management. In: Nejadkoorki, Farhad (Ed.), Advance in Air Pollution. Intech, pp. 429–454.
Rentziou, A., Gkritza, K., Souleyrette, R., 2012. VMT, energy consumption, and GHG emissions forecasting for passenger transportation. Transp. Res. Part A 46, 487–500.
Scire, J.S., Strimaitis, D.G., Yamartino, R.J., 2000. A User's Guide for the CALPUFF Dispersion Model. Concord, MA.
Singer, B.C., Harley, R.A., 1996. A fuel-based motor vehicle emission inventory. J. Air Waste Manag. Assoc. 46, 581–593.
Souleyrette, R.R., Sathisan, S.K., James, D.E., Lim, S., 1992. GIS for transportation and air quality analysis. In: Proceedings of the National Conference on Transportation Planning and Air Quality. ASCE, New York, NY, pp. 182–194.
Uherek, E., Halenka, T., Borken-Kleefeld, J., Balkanski, Y., Berntsen, T., Borrego, C., Gauss, M., Hoor, P., Juda-Rezler, K., Lelieveld, J., Melas, D., Rypdal, K., Schmid, S., 2010. Transport impacts on atmosphere and climate: land transport. Atmos. Environ. 44, 4772–4816.
UN, 2010. United Nations. Energy Statistics Yearbook. UN, NY, USA.
Wang, S., Zhenga, J., Fua, F., Yina, S., Zhong, L., 2011. Development of an emission processing system for the Pearl River Delta Regional air quality modeling using the SMOKE model: methodology and evaluation. Atmos. Environ. 45, 5079–5089.
Yan, X., Crookes, R., 2009. Reduction potentials of energy demand and GHG emissions in China's road transport sector. Energy Policy 37, 658–668.
Zhang, K., Batterman, S., 2010. Near-road air pollutant concentrations of CO and PM2.5: a comparison of MOBILE6.2/CALINE4 and generalized additive models. Atmos. Environ. 44, 1740–1748.